Eur Phys J C **33**, s01, s107–s113 (2004)
Digital Object Identifier (DOI) 10.1140/epjcd/s2004-03-1665-y

EPJ C direct
electronic only

Relativistic heavy ion physics: An experimental review

Saskia Mioduszewski

Physics Department, Brookhaven National Laboratory, Upton, NY 11973

Received: 9 January 2004 / Accepted: 26 January 2004 /
Published Online: 25 February 2004 –

Abstract. A review of relativistic heavy ion physics is given, with emphasis on selected interesting results. The charged particle multiplicity is compared from measurements at the AGS, SPS, and RHIC. Collective motion due to a build-up of pressure is discussed, with implications on estimates of the energy density of the produced medium. The suppression of J/ψ and the enhancement of low-mass dileptons observed in experiments at the SPS are highlighted. The high p_T phenomena at RHIC are discussed in some detail. The suppression of high p_T hadrons in central Au+Au collisions is shown, as well as the absence of such a suppression in d+Au collisions.

PACS. 25.75.-q Relativistic heavy-ion collisions

1 Introduction

Numerical simulations of quantum chromodynamics (QCD) on a lattice predict a phase transition from hadronic matter to deconfined, chirally symmetric matter at sufficiently large energy densities [1]. The critical energy density calculated is typically ~ 0.7 GeV/fm^3, approximately 5 times the density of normal nuclear matter. The primary goal of high energy heavy ion physics is to achieve such a phase transition and to study this new state of matter, the Quark Gluon Plasma (QGP). This field has recently entered a new energy regime with the Relativistic Heavy Ion Collider (RHIC) at BNL. In the 1980's and 1990's, experiments were performed at the AGS (BNL), at center of mass energies $\sqrt{s_{NN}} \sim 5$ GeV, and at the SPS (CERN) at $\sqrt{s_{NN}} \sim 20$ GeV with fixed targets. With the new collider, energies of $\sqrt{s_{NN}} \sim 200$ GeV have been reached.

To identify the Quark Gluon Plasma in heavy ion collisions, we have been given several tools from theory. Among them are the suppression of J/ψ as a signature of deconfinement [2], the quenching of jets in the medium as an indication of large densities [3], thermally produced direct photons or dileptons to extract the temperature of the medium in the hot/dense phase [4], the dilepton continuum at low invariant masses to study chiral symmetry restoration [5], and collective flow as an indication of equilibration of the system [6]. Here we review results from several of these topics. In Sect. 2, we present the charged particle multiplicities over a range of system energies and discuss radial and elliptic flow. Then in the following sections, we have chosen to highlight three particularly compelling results from the field of relativistic heavy ion physics. The first is J/ψ suppression, and the second is low-mass dilepton enhancement, both observed at the SPS. The third is high p_T hadron suppression, which was a new discovery at RHIC. Finally, a summary of this review is given in Sect. 6.

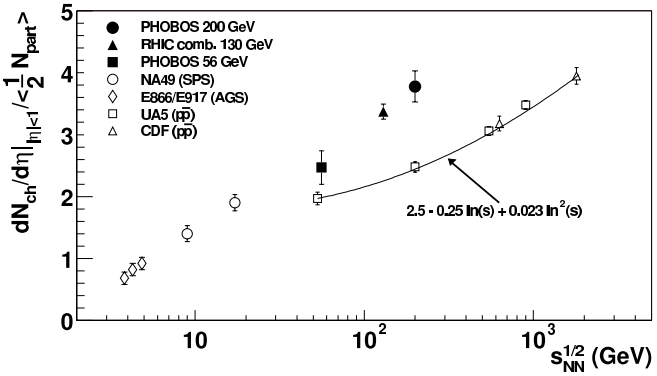

Fig. 1. $dN_{ch}/d\eta$ per participant pair vs. $\sqrt{s_{NN}}$ [7]

2 Global observables

In relativistic heavy ion physics, a common way to present observables is as a function of the centrality of the colliding nuclei. The properties of the medium produced in a collision depend on the centrality. Events are divided into selections by percentiles of the total cross section, which can be characterized by a mean impact parameter, a mean number of participating nucleons N_{part}, and a mean number of binary nucleon-nucleon collisions N_{binary}. In this section, we present data on charged particle multiplicities to provide a general idea of the amount of entropy produced in these collisions. Then we discuss the collective motion or "flow" of the system produced in the collisions.

Send offprint requests to: Saskia Mioduszewski

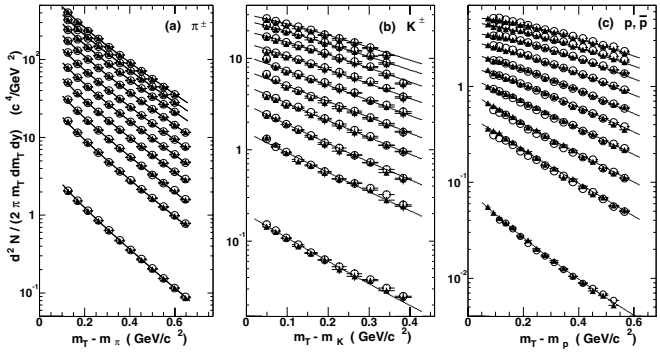

Fig. 2. Invariant yields of identified hadrons as a function of m_T for the most central collisions to peripheral, from *top* to *bottom* [13]. The *bottom* spectrum in each panel is measured in p+p collisions

2.1 Charged particle multiplicity

The charged particle multiplicity is a basic observable which provides input to theoretical models to help constrain the initial conditions. Figure 1 shows the pseudorapidity density of charged particles, $dN_{ch}/d\eta$, per participant pair as a function of $\sqrt{s_{NN}}$ for central heavy ion collisions (Pb+Pb and Au+Au) [7,8,9] and p+$\overline{p}$ collisions [10, 11].

At RHIC, the number of participants N_{part} is approximately 350 for the most central collisions, so there are more than 650 charged particles per unit of pseudorapidity at mid-rapidity. The charged particle multiplicity per participant in the heavy ion data increases logarithmically with $\sqrt{s_{NN}}$. From SPS at $\sqrt{s_{NN}} \sim 20$ GeV to RHIC at 200 GeV, there is a factor of two increase. The increase with energy is faster than the increase observed in $p + \overline{p}$ collisions. It is also interesting to note that the charged particle multiplicity per participant at RHIC is significantly larger ($\sim 65\%$) than that measured in $p + \overline{p}$ collisions at the same energy. This rules out simple models in which particle production scales with the the number of participants N_{part} [12]. The stronger increase with energy in central heavy ion collisions may be explained by the increasing role of hard processes (which scale with N_{binary}) with increasing collision energy. The role of hard processes at RHIC will be discussed in more detail in Sect. 5.

2.2 Flow

Heavy ion collisions create large, coherently interacting systems in which the particles can undergo numerous rescatterings leading to a build-up of pressure. Radial flow is the term used to denote the collective expansion of the system driven by pressure. If the matter elements move with a common velocity, then heavier particles will be shifted to higher transverse momenta. Thus, the flow velocity can be deduced by examining transverse momentum spectra for particles of different masses. Figure 2 shows the transverse mass spectra of charged particles measured by the STAR experiment [13].

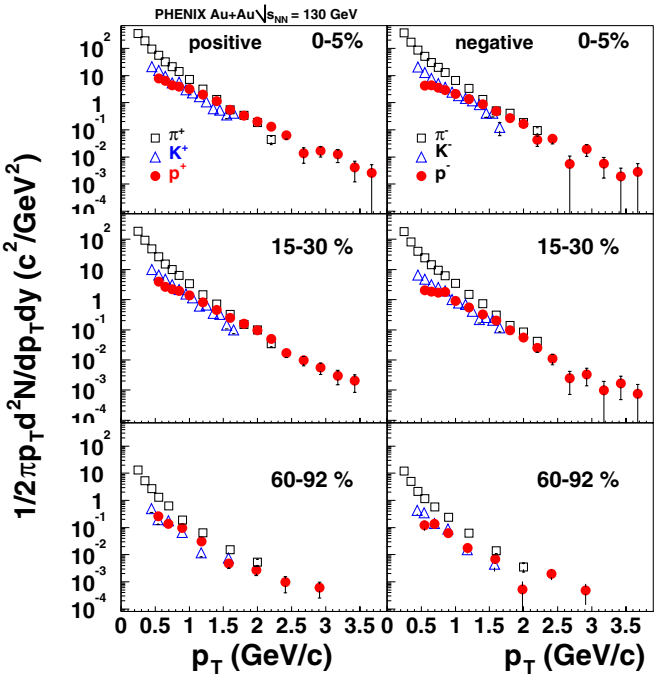

Fig. 3. Invariant yields of identified hadrons as a function of p_T for the most central collisions to peripheral, from *top to bottom panels* [14]

The proton spectra are flatter than the pion and kaon spectra, and they systematically become flatter with increasing centrality. Figure 3 shows the transverse momentum spectra, measured by the PHENIX experiment [14], for identified hadrons in collisions at $\sqrt{s_{NN}} = 130$ GeV in a higher p_T range than the previous figure.

The spectra can be described by hydrodynamic models up to 2-3 GeV/c for baryons and 1-2 GeV/c for mesons. Hydrodynamics is not expected to be valid at high p_T because fast particles escape the system before they have enough reinteractions to thermalize. It also breaks down for peripheral collisions where the system size is too small, and again the particles can escape before thermalization. With a blast-wave model [15], a hydrodynamically motivated model, one can extract the freeze-out temperature T_{fo} and transverse expansion velocity β_T by fitting the 3 particle species simultaneously. At the SPS, such fits produce $T_{fo} \sim 120 - 130$ MeV and $\beta_T \sim 0.4 - 0.5$, and at RHIC, $T_{fo} \sim 100 - 110$ MeV and $\beta_T \sim 0.5 - 0.6$. The protons and pions in Fig. 3 become comparable in magnitude at $p_T \sim 2$ GeV/c. This is not expected from particle production due to hard scattering and fragmentation. However, it is in good agreement with the expectation from hydrodynamics [16], where heavier particles are shifted to higher p_T. Other recent theoretical explanations of the large proton content at $p_T \sim 2$ GeV/c include coalescence models [17,18,19,20], in which the coalescence of quarks rivals parton fragmentation as the production mechanism in this p_T range.

Another important observable characterizing the collective expansion is the azimuthal anisotropy, known as elliptic flow. While radial flow is largest in the most cen-

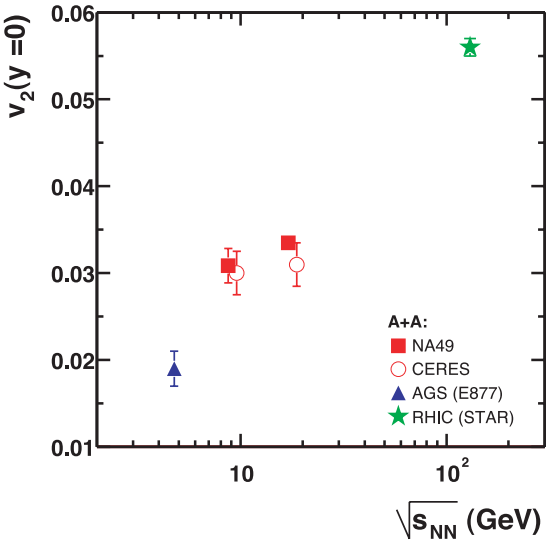

Fig. 4. v_2, averaged over p_T, measured in *mid-central* collisions, shown as a function of $\sqrt{s_{NN}}$ [21]

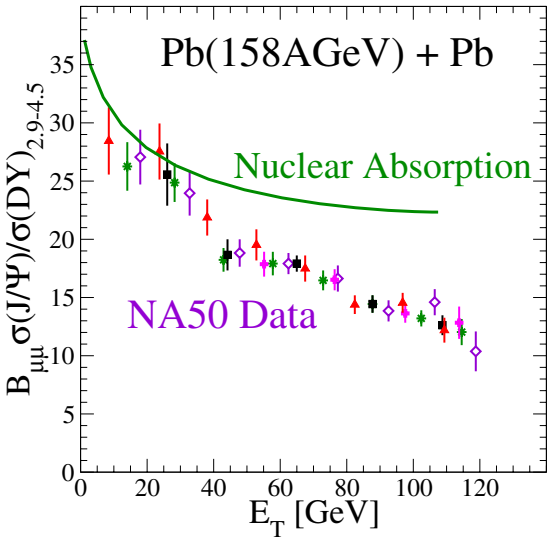

Fig. 5. NA50 J/ψ cross section scaled by the Drell-Yan cross section (for di-muons with invariant mass in the range 2.9-4.5 GeV/c^2) as a function of E_T. The data from different analyses [30] are shown in different colors. The *line* shows the expectation of the suppression as a function of E_T assuming the nuclear absorption cross section that is measured in p+Au collisions

tral collisions, elliptic flow depends on the initial asymmetry of the system and is thus largest for non-central collisions. In a non-central collision, the region of interaction is almond-shaped. With enough reinteraction, the system builds up pressure transforming the initial asymmetry present in coordinate space into a momentum anisotropy. In order for such a momentum anisotropy to be observed, the pressure must build up before the system has expanded and the initial asymmetry has disappeared. Therefore, the elliptic flow reflects the amount of reinteraction in the early times of the collision dynamics. To quantify the azimuthal anisotropy, we measure the second coefficient v_2 in a Fourier expansion in ϕ of the particle spectrum $d^2N/p_T dp_T d\phi$, where ϕ is measured with respect to the reaction plane determined for each event. Figure 4 shows the v_2 measured at different energies from the AGS to RHIC [21,22,23,24].

The elliptic flow v_2 was measured to be ~ 0.03 in mid-central collisions at the SPS, and ~ 0.06 at RHIC. This is a larger increase than expected, and it suggests early equilibration at RHIC [25]. From hydrodynamical models, the equilibration time may be as fast as 0.6 fm/c. This has an interesting implication on the energy density. Using the Bjorken formula [26],

$$\epsilon = \frac{1}{\pi R^2 \tau_0} \frac{dE_T}{dy}, \qquad (1)$$

combined with the measurement for transverse energy, $dE_T/dy \sim 720$ GeV at $\sqrt{s_{NN}} = 200$ GeV [27], and the equilibration time estimated from hydrodynamical models, $\tau_0 = 0.6$ fm/c, the energy density is approximately 8 GeV/fm^3. Using a more conservative τ_0 of 1 fm/c, the energy density is ~ 5 GeV/fm^3. At the SPS, similar estimates of the energy density, assuming $\tau_0 = 1$ fm/c, are typically ~ 2.5 GeV/fm^3. Such estimates are well above the predictions for the critical energy density from lattice QCD (see Sect. 1).

3 J/ψ production and suppression

It was predicted that the formation of the Quark Gluon Plasma would lead to a suppression of J/ψ [2]. The J/ψ are expected to dissociate and the charm quarks to be color-screened in the deconfined medium, leading to fewer observed J/ψ [28]. Such a suppression was discovered in Pb+Pb collisions at the SPS [29]. Figure 5 shows the measured J/ψ divided by the Drell-Yan cross section as a function of E_T, or centrality [30]. The Drell-Yan cross section was shown to scale with the number of binary nucleon-nucleon collisions ("binary scaling"), and thus provides the reference for the J/ψ measurement. The ratio decreases with respect to centrality, showing that the J/ψ cross section is suppressed in more central collisions relative to binary scaling. NA50 measured the absorption cross section in p+Au collisions to be (4.4 ± 0.5) mb [31]. The suppression in excess of the expectation from "normal" nuclear absorption (shown as a solid line in Fig. 5) is referred to as "anomalous" J/ψ suppression.

Although the J/ψ suppression may be the most compelling evidence for the formation of the QGP at SPS, at RHIC the theory has a possible additional component. On the one hand, the J/ψ is expected to be more suppressed than at the SPS because the energy density is larger. On the other hand, there are significantly more $c\bar{c}$ pairs produced initially in collisions at RHIC energies, allowing for the possibility of recombination of pairs to form more J/ψ at a later stage [32,33,34,35]. A first measurement at RHIC was made by the PHENIX experiment [36], but the statisics are very limited. Figure 6 shows the J/ψ yield scaled by N_{binary} as a function of the number of participants N_{part}, or centrality. With the available statis-

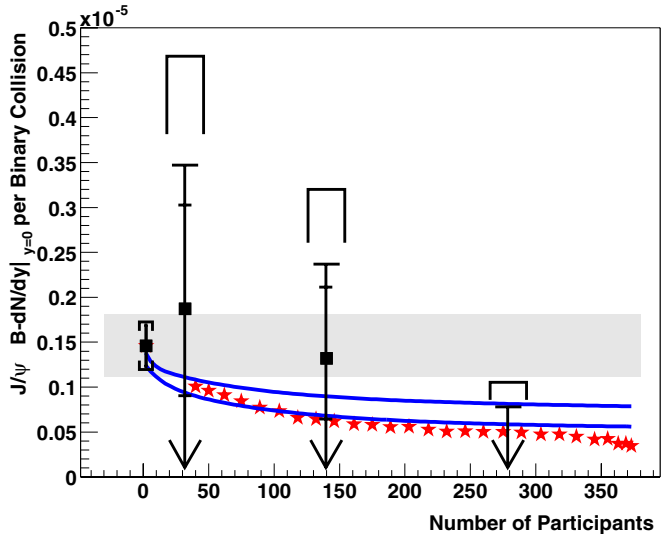

Fig. 6. PHENIX J/ψ yields scaled by N_{binary} as a function of N_{part} [36]. The *shaded band* represents the expectation from binary scaling. See *text* for a description of *lines and stars*

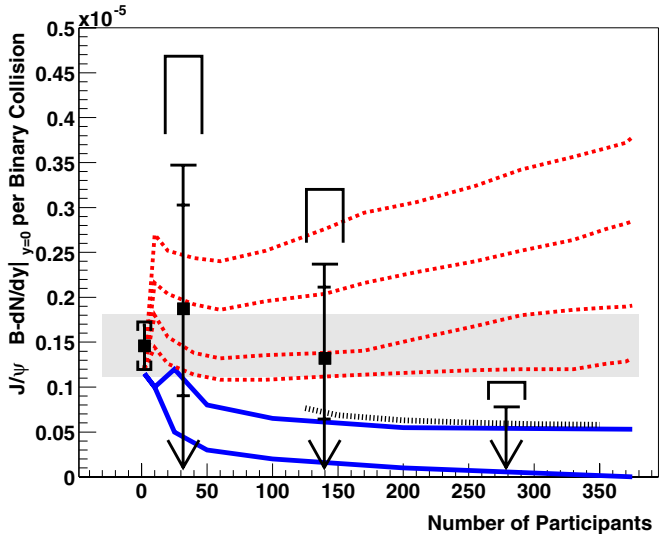

Fig. 7. PHENIX J/ψ yields scaled by N_{binary} as a function of N_{part} compared to theoretical models. See *text* for a description of the *lines*

tics, the Au+Au data was divided into 3 centrality selections and compared to the p+p data. The data point at $N_{part} = 2$ is a measurement from the p+p reactions in the same experiment [37], and the shaded band around this data point denotes the expectation from binary scaling within uncertainties. The p+p measurement is an important baseline for the Au+Au measurement. The stars show the NA50 suppression normalized to the PHENIX p+p data point. The 2 solid lines show the expectation from normal nuclear absorption, assuming 2 different absorption cross sections. RHIC has recently provided d+Au collisions at $\sqrt{s_{NN}} = 200$ GeV. The J/ψ measurement in d+Au collisions is important to determine the nuclear absorption cross section at this energy.

Figure 7 shows the same data compared to theoretical models.

The 4 upper red dashed lines are from a plasma coalescence model assuming 4 different charm rapidity widths [33]. The lower blue solid line is a calculation with absorption in the nuclear medium and in the plasma, while the upper also includes the regeneration of J/ψ assuming the equilibration of charm [35]. The hashed line is a statistical model [38]. The comparison leads to the conclusion that models predicting a large enhancement relative to binary scaling are not supported by the data. However, the data cannot discriminate between different models that lead to a suppression. This coming run at RHIC is expected to provide much increased luminosity which will improve this measurement.

4 Low-mass dileptons

Another compelling result from the SPS is the large excess of low-mass dilepton production. The CERES experiment measured a strong enhancement of low-mass dileptons in Pb+Au collisions relative to the yield expected

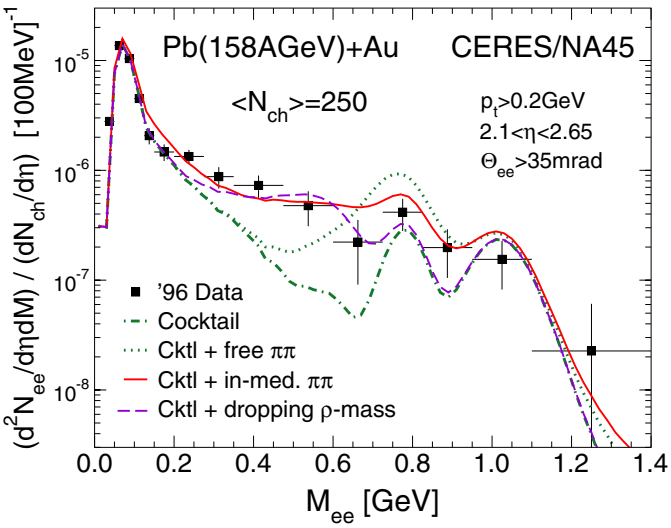

Fig. 8. CERES di-electron yields vs. invariant mass compared to different calculations [39]. See *text* for discussion of calculations

from known sources [39]. Figure 8 shows the yield of e^+e^- pairs as a function of their invariant mass. The dashed-dotted green line is the cocktail calculation, based on the decays of produced hadrons. The enhancement is a factor of $2.6 \pm 0.5(stat.) \pm 0.6(syst.)$ in the mass region between 250 and 700 MeV/c^2.

It should be noted that in p+Au collisions the measurement was found to be consistent with the hadron decay cocktail [40]. The theoretical interpretation of the enhancement requires a thermal source of $\pi\pi$ annihilation, in the hadron gas phase of the collision, contributing to the yield of dileptons through the ρ-meson channel. But in order to reproduce the invariant mass dependence of the enhancement, the leading theoretical interpretations in-

voke medium modifications of this thermal source [41,42]. Two different approaches that have been proposed are the broadening of the spectral function of the ρ-meson mass distribution [42] and the dropping of the ρ-meson mass [41] due to interactions in the hot and dense hadronic medium. The dotted green line in Fig. 8 is the cocktail calculation with additional production from the thermal source, but calculated with the free line-shape of the ρ spectral function. The red solid line denotes the total yield as a function of invariant mass from invoking the broadening of the ρ spectral function, and the purple dashed line from invoking the dropping mass of the ρ. The connection to chiral symmetry restoration is that the chiral partner of the ρ is the a_1-meson. Both theoretical approaches can, in principle, lead to degenerate states of the a_1 and the ρ (although it has not been explicitly shown for the broadening approach), and both calculations reproduce the data. This measurement, which will also be made at RHIC, will hopefully give insight to how chiral symmetry is restored.

5 High p_T hadrons

At sufficiently high transverse momenta, particle yields are dominated by the production of jets from hard scatterings. In p+p collisions, it is known that hard scattering and the fragmentation of the scattered partons dominates the production of hadrons above $p_T \sim 2$ GeV/c [43]. In heavy ion collisions, the boundary between where hard and where soft production dominates the measured hadron yields is affected by flow [16,6] and possibly parton coalescence [17,18,19,20]. In Run II at RHIC ($\sqrt{s_{NN}} = 200$ GeV), hadrons have been measured up to $p_T \sim 10$ GeV/c in Au+Au collisions [44,45] and in p+p collisions [46]. At such large transverse momenta, particle are expected to undergo incoherent interactions even in heavy ion collisions, and perturbative QCD calculations can reliably be used as a baseline for hadron production [47,48,49,50].

In a heavy ion collision hard scattering occurs early, before the hot, dense phase is formed. A hard scattering occurs on a timescale of $\sim 1/p_T$, which for $p_T = 2$ GeV is approximately 0.1 fm/c. This is smaller than the equilibration time (see Sect. 2). Therefore, the hard-scattered partons experience the entire space-time of the system and serve as a probe of the produced medium. It has been predicted that the hard-scattered partons will reinteract in a deconfined medium of free color charges, losing much of their energy [3]. This would result in a suppression of the high transverse momentum tail of the hadron spectrum, where a hadron is likely to be the leading particle of a jet. We generally measure the effects of the nuclear medium by comparing the yields at high p_T measured in A+A collisions to those measured in p+p collisions scaled by the number of binary nucleon-nucleon collisions N_{binary}.

$$R_{AA}(p_T) = \frac{(\text{Yield per A + A collision})}{\langle N_{binary}\rangle(\text{Yield per p + p collision})} = \frac{d^2N^{A+A}/dp_T d\eta}{\langle N_{binary}\rangle(d^2\sigma^{p+p}/dp_T d\eta)/\sigma^{p+p}_{inelastic}}. \quad (2)$$

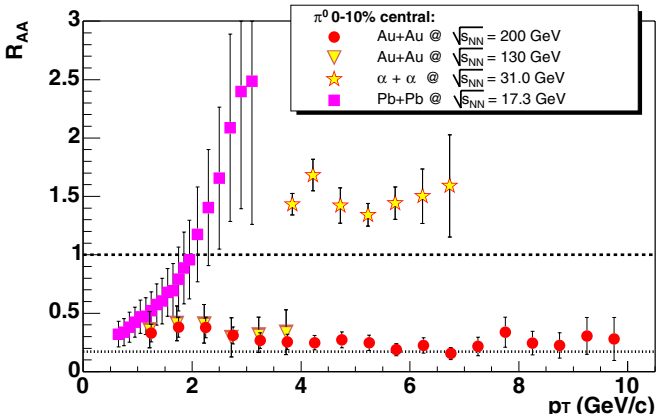

Fig. 9. R_{AA} for neutral pions in central Au+Au collisions at RHIC [56,44], central Pb+Pb collisions at the SPS [55] ($\sqrt{s_{NN}} = 17$ GeV), and α+α collisions [54] ($\sqrt{s_{NN}} = 31$ GeV)

At low p_T, where soft production dominates the measured yields, R_{AA} is less than one because soft production is expected to scale with the number of participants N_{part}, rather than N_{binary}. At transverse momenta sufficiently large to be in a hard-scattering regime and in the absence of any nuclear effects, R_{AA} is expected to be equal to unity. In this case, an A+A collision can simply be described as a superposition of binary N+N collisions. A deviation from unity at high p_T is a measure of the effect of the nuclear medium. Previously measured nuclear effects include the "Cronin" effect [51], an enhancement in the yields relative to binary scaling attributed to k_T broadening due to initial state multiple scattering [52,53]. The predicted energy loss due to the dense medium is a suppression, known as "jet quenching." Figure 9 shows the measured R_{AA} for neutral pions in α+α collisions at $\sqrt{s_{NN}} = 31$ GeV [54], in Pb+Pb collisions at $\sqrt{s_{NN}} = 17$ GeV at the SPS [55], and in Au+Au collisions at $\sqrt{s_{NN}} = 130$ GeV [56] and $\sqrt{s_{NN}} = 200$ GeV [44] at RHIC.

In $\alpha + \alpha$ collisions, the system size is small, and the effect of energy loss is not expected. However an effect of the nuclear medium is present and is observed as the Cronin effect. At the SPS, in Pb+Pb collisions, there is no apparent suppression, and any possible energy loss effect present in these collisions is completely dominated by the Cronin effect. At RHIC, for the first time, a suppression was observed in central Au+Au collisions in Run I for p_T between 2 and 4 GeV/c [56], consistent with the prediction for jet quenching. The suppression persisting up to $p_T = 10$ GeV/c, observed in Run II, was successfully predicted by theoretical calculations that invoke an energy loss proportional to the energy of the parton combined with shadowing and initial-state k_T-broadening [57, 58]. Important to note is that the suppression is not observed in peripheral Au+Au collisions at RHIC, but that the measured hadron yields in peripheral collisions are consistent with the binary-scaled yields measured in p+p collisions, i.e. R_{AA} is consistent with unity [44].

Due to the high multiplicity environment, jets cannot be directly observed in a heavy ion collision. When interpreting the modification of the particle spectra at high p_T

as an effect of the medium on the hard-scattered partons, one assumes that the hadrons measured at high p_T emanate from jets. A method to detect the presence of jets in high multiplicity environment is via two-particle angular correlation measurements. To extract the jet signal from the correlation distributions, other sources of correlation, such as flow and resonance decays, and the combinatorial background need to be disentangled from the correlations due to jets. The STAR experiment has made such a measurement [59] and found that the away-side jet disappears in central Au+Au collisions. This is shown in the bottom right panel of Fig. 10. The "near-side" correlations are those at $|\Delta\phi| \sim 0°$, and the "away-side" are at $|\Delta\phi| \sim 180°$. Since the near-side contains the trigger particle, the correlation function can be understood as a conditional probability. When triggering on a high p_T particle, the near-side correlation looks very similar to the correlation due to jets measured in p+p collisions (black histogram); but there is no jet correlation seen on the away-side, contrary to what is measured in p+p collisions. A possible interpretation is that the hadrons that we measure at high p_T in central Au+Au collisions come from hard scatterings near the surface of the system. This would allow one jet to escape the medium; while the corresponding jet must traverse the dense medium where it could interact, lose much its energy, and become lost in the low p_T soft part of the spectrum. Although both of these observations that were made in central Au+Au collisions at RHIC (the suppression in the hadron spectrum at high p_T and the disappearance of the away-side jet) seem to indicate that the hard-scattered partons lose energy in the dense medium, the effect of the "cold" nuclear medium (p+A or d+A collisions) had to be measured to rule out initial-state nuclear effects.

In Run III at RHIC, high p_T particle production was studied in d+Au collisions. To distinguish initial-state effects from final-state effects on the suppression observed in central Au+Au collisions, d+Au collisions provide a good comparison experiment with only initial-state nuclear effects. Figure 10 shows the results from all 4 RHIC experiments [60,61,62,63].

From these results, the consistent conclusion is that the suppression observed in central Au+Au collisions is not observed in d+Au collisions. Similarly, the disappearance of the away-side jet (bottom right panel) is also not observed in d+Au collisions.

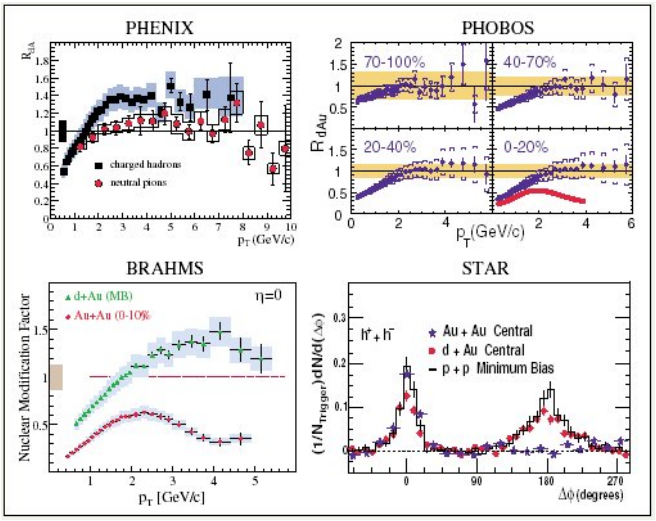

Fig. 10. Results of measurements in d+Au collisions from all 4 RHIC experiments as a comparison to the novel effects observed in central Au+Au collisions. The two upper and the *lower left* panel show R_{AA} vs. p_T, and the *bottom right* panel shows the angular correlation measurement due to jets. The *upper left* shows R_{AA} for neutral pions and charged hadrons measured in d+Au collisions by PHENIX [60]. The *upper right* shows R_{AA} for charged hadrons measured in different centrality selections in d+Au collisions by PHOBOS [61], where the most central in d+Au collisions is compared to the measurement in central Au+Au collisions (*the red line*). The *lower left* is R_{AA} in d+Au collisions compared to central Au+Au collisions measured by BRAHMS [62]. The *lower right* is the jet correlation signal measured in p+p collisions, d+Au collisions, and central Au+Au collisions by STAR [63]

6 Summary

Results from the relativistic heavy ion program show that we are producing conditions that are necessary, although perhaps not sufficient, for the formation of the Quark Gluon Plasma. Flow measurements show that there is significant pressure in heavy ion collisions both at the SPS and at RHIC. The transverse expansion velocity of the system is found to be $\beta_T = 0.4-0.5$ at SPS and $\beta_T = 0.5-0.6$ at RHIC. The large elliptic flow at RHIC, moreover, is evidence pointing to early equilibration, perhaps as early as 0.6 fm/c, according to hydrodynamic models. Such estimates of the equilibration time imply a large energy density. The energy density at RHIC is approximately 5 GeV/fm^3, even assuming a conservative equilibration time, $\tau_0 = 1$ fm/c. This is almost an order of magnitude larger than the critical energy density for the phase transition as predicted by lattice QCD.

Among the highlights at the SPS, the NA50 experiment observed an anomalous J/ψ suppression in Pb+Pb collisions increasing with centrality. The suppression exceeds that from normal nuclear absorption and is consistent with predictions due to deconfinement. The CERES experiment observed an enhancement in low-mass dileptons in the mass range between 250 and 700 MeV/c^2. Such an observation is consistent with a thermal source of dileptons with large medium modifications on the ρ-meson.

At RHIC, after the first three runs, one of the most significant observations thus far is the depletion of high p_T hadrons in central Au+Au collsions. Such a suppression is consistent with predictions in which hard-scattered partons lose energy in a dense medium. Complementing this observation is the discovery of the disappearance of the away-side jet in central Au+Au collisions, which also supports the explanation of interactions of the hard-scattered partons in a dense medium. As a reference for the effect of cold nuclear matter on hadron spectra at high p_T and

on correlations due to jets, the same measurements were made in d+Au collisions. The charged hadron and neutral pion spectra were not found to be suppressed relative to the binary-scaled spectra measured in p+p collisions, and the away-side jet did not disappear. This indicates that the novel phenomena observed in central Au+Au collisions at RHIC are due to effects of the medium produced in these collisions, rather than initial-state nuclear effects.

All of these results are interesting effects observed in heavy ion collisions. However, evidence for the achievement of a phase transition is not conclusive. There is much to be learned about the dynamics of these collisions and the properties of the produced medium. Further studies of the high p_T phenomena, and the competition between soft and hard processes at intermediate p_T, will be performed at RHIC. Measurements of J/ψ and dilepton/photon production will also be important for a better understanding of the medium produced in heavy ion collisions.

Acknowledgements. I would like to thank the organizers for the invitation to this interesting and pleasant conference. I acknowledge support for this work from the Department of Energy.

References

1. See E. Laermann and O. Philipsen: hep-ph/0303042 (to appear in Ann. Rev. Nuc. Part. Sci.), for a recent review
2. T. Matsui and H. Satz: Phys. Lett B **178**, 416 (1986)
3. M. Gyulassy and M. Plümer: Phys. Lett. B **243**, 432 (1990); X.N. Wang and M. Gyulassy: Phys. Rev. Lett. **68**, 1480 (1992); R. Baier et al.: Phys. Lett. B **345**, 277 (1995)
4. E. Shuryak: Phys. Rep. **61**, 72 (1980)
5. See R. Rapp and J. Wambach: Adv. Nucl. Phys. **25**, 1 (2000), for a review
6. See P.F. Kolb and U. Heinz: nucl-th/0305084, for a recent review
7. B.B. Back et al.: Phys. Rev. Lett. **88**, 22302 (2002)
8. J. Bächler et al.: Nucl. Phys. A **661**, 45 (1999); C. Blume et al.: Nucl. Phys. A **698**, 104-111 (2002)
9. L. Ahle et al.: Phys. Lett. B **476**, 1 (2000); Phys. Lett. B **490**, 53 (2000)
10. F. Abe et al.: Phys. Rev. D **41**, 2330 (1990)
11. G.J. Alner et al.: Z. Phys. C **33**, 1 (1986)
12. A. Bialas, B. Bleszynski, and W. Czyz: Nucl. Phys. B **111**, 461 (1976)
13. J. Adams et al.: nucl-ex/0310004
14. K. Adcox et al.: Phys. Rev. Lett. **88**, 242301 (2002)
15. E. Schnedermann, J. Sollfrank, and U. Heinz: Phys. Rev. C **48**, 2462 (1993)
16. D. Teaney, J. Lauret, and E.V. Shuryak: nucl-th/0110037
17. R.C. Hwa and C.B. Yang: Phys. Rev. C **67**, 034902 (2003)
18. R.J. Fries, B. Müller, C. Nonaka, and S.A. Bass: Phys. Rev. Lett. **90**, 202303 (2003)
19. V. Greco, C.M. Ko, and P. Levai: nucl-th/0301093
20. D. Molnar and S.A. Voloshin: Phys. Rev. Lett. **91**, 092301 (2003)
21. A. Wetzler et al.: Nucl. Phys. A **715**, 583-586 (2003)
22. S.A. Voloshin and A.M. Poskanzer: Phys. Lett. B **474**, 27-32 (2000)
23. K. Filimonov et al.: INPC (2001), nucl-ex/0109017
24. C. Adler et al.: Phys. Rev. C **66**, 034904 (2002)
25. U.W. Heinz and P.F. Kolb: Nucl. Phys. A **702**, 269-280 (2002)
26. J.D. Bjorken: Phys. Rev. D **27**, 140 (1983)
27. A. Bazilevsky et al.: Nucl. Phys. A **715**, 486 (2003)
28. D. Kharzeev et al.: Z. Phys. C **74**, 307 (1997); J.P. Blaizot, P.M. Dinh, and J.Y. Ollitrault: Phys. Rev. Lett. **85**, 4012 (2000)
29. NA50 Collaboration: Phys. Lett. B **410**, 337 (1997)
30. NA50 Collaboration (L. Ramello et al.): Nucl. Phys. A **715**, 243 (2003)
31. NA50 Collaboration: Phys. Lett. B **553**, 167-178 (2003)
32. P. Braun-Munzinger and J. Stachel: Phys. Lett. B **490**, 196 (2000)
33. R.L. Thews, M. Schroedter, and J. Rafelski: Phys. Rev. C **63**, 054905 (2001); R.L. Thews: Strange Quark Matter 2003 conference proceedings
34. M.I. Gorenstein et al.: Phys. Lett. B **509**, 277 (2001)
35. L. Grandchamp and R. Rapp: Phys. Lett. B **523**, 60 (2001); Nucl. Phys. A **709**, 415 (2002)
36. S.S. Adler et al.: nucl-ex/0305030, to appear in Phys. Rev. C
37. S.S. Adler et al.: hep-ex/0307019, to appear in Phys. Rev. Lett
38. A. Andronic et al.: nucl-th/0303036
39. G. Agakichiev et al.: Phys. Lett. B **422**, 405 (1998)
40. G. Agakichiev et al.: Eur. Phys. J C **4**, 231 (1998)
41. G.E. Brown and M. Rho: Phys. Rev. Lett. **66**, 2720 (1991); G.E. Brown and M. Rho: Phys. Rep. **269**, 333 (1996)
42. R. Rapp, G. Chanfray, and J. Wambach: Nucl. Phys. A **617**, 472 (1997)
43. J.F. Owens et al.: Phys. Rev. D **18**, 1501 (1978)
44. S.S. Adler et al.: Phys. Rev. Lett **91**, 072301 (2003)
45. J. Adams et al.: nucl-ex/0305015, submitted to Phys. Rev. Lett
46. S.S. Adler et al.: hep/ex/0304038, submitted to Phys. Rev. Lett
47. I. Vitev and M. Gyulassy: Phys. Rev. Lett **89**, 252301 (2002)
48. S. Jeon, J. Jalilian-Marian, and I. Sarcevic: Phys. Lett. B **562**, 45 (2003)
49. G.G. Barnafoldi et al.: nucl-th/0212111
50. X.N. Wang: Nucl. Phys. A **715**, 775 (2003)
51. D. Antreasyan et al.: Phys. Rev. D **19**, 764 (1979)
52. M. Lev and B. Petersson: Z. Phys. C **21**, 155 (1983); T. Ochiai et al.: Prog. Theor. Phys. **75**, 288 (1986)
53. X.N. Wang: Phys. Rev. C **61**, 064910 (2000)
54. A.L.S. Angelis et al.: Phys. Lett. B **185**, 213 (1987)
55. M.M. Aggarwal et al.: Eur. Phys. J **23**, 225 (2002)
56. K. Adcox et al.: Phys. Rev. Lett. **88**, 022301 (2002)
57. P. Levai et al.: Nuclear Physics A **698**, 631 (2002)
58. I. Vitev and M. Gyulassy: Phys. Rev. Lett. **89**, 252301 (2002)
59. C. Adler et al.: Phys. Rev. Lett. **90**, 082302 (2003)
60. S.S. Adler et al.: Phys. Rev. Lett. **91**, 072303 (2003);
61. B.B. Back et al.: Phys. Rev. Lett. **91**, 072302 (2003)
62. I. Arsene et al.: Phys. Rev. Lett. **91**, 072305 (2003)
63. J. Adams et al.: Phys. Rev. Lett. **91**, 072304 (2003)